

Design and Demonstration of an Interference Suppressing Microwave Radiometer

Grant A. Hampson, Steven W. Ellingson*, and Joel T. Johnson
The Ohio State University ElectroScience Laboratory
1320 Kinnear Rd., Columbus, OH 43212
{hampson.8, johnson.1374}@osu.edu

*Department of Electrical and Computer Engineering
Virginia Tech
340 Whittemore Hall, Blacksburg, VA 24061
ellingson@vt.edu

Abstract— Microwave radiometers operating outside protected portions of the frequency spectrum can be adversely impacted by radio frequency interference. In this paper, we describe a new radiometer which coherently samples 100 MHz of spectrum and applies real-time RFI mitigation techniques using FPGAs. A field test of an interim version of this design in a radio astronomy observation corrupted by radar pulses is described. Experiments currently in progress to demonstrate the system in ground-based remote sensing are also detailed.

Since December 2001, we have been working to develop such a radiometer. Our design, described in Section 2, is capable of coherently sampling 100 MHz, with real-time RFI mitigation implemented using field-programmable gate array (FPGA) devices. In Section 3, we describe a test of an interim implementation of our design in an L-band radio astronomy application, while Section 4 provides information on ground-based remote sensing demonstrations currently in progress. To provide additional information on the radio frequency interference environment at L-band, we have also been performing surveys with an airborne instrument. Survey results and plans for operations at C-band are described in Section 5.

TABLE OF CONTENTS

- 1 INTRODUCTION
- 2 RADIOMETER DESIGN
- 3 ON-THE-AIR TESTING AT ARECIBO
- 4 REMOTE SENSING EXPERIMENTS
- 5 RFI SURVEYS
- 6 IMPLICATIONS

1. INTRODUCTION

Radio frequency interference (RFI) can adversely impact the performance of microwave radiometers operating outside protected portions of the frequency spectrum. For L-band systems, 27 MHz is protected from 1400-1427 MHz, but bandwidths on the order of 100 MHz are desirable to improve sensitivity in applications such as soil moisture and ocean salinity sensing. No protected spectrum is available at C-band, and results from the C-band channel of the AMSR-E sensor on the AQUA satellite are showing significant RFI induced corruption of data [1]. Because much of the RFI at L-band band is from radars with pulse lengths on the order of microseconds, traditional radiometers (i.e., those which directly measure total power integrated over time scales of milliseconds or greater) are poorly suited to mitigating these contributions. This motivates the design and development of radiometers capable of coherent sampling and adaptive, real-time mitigation of interference.

2. RADIOMETER DESIGN

A block diagram of our radiometer is shown in Figure 1, and a picture of the digital section is shown in Figure 2. The analog front end downconverts an 80 MHz swath of spectrum from L-band to 150 MHz, and samples this signal at 200 MSPS using 10 bits. Note the system can also be operated at frequencies other than L-band simply by modifying the analog front end and downconverter sections. Because the analog IF is in the second Nyquist zone of the A/D, the digital passband is centered at 50 MHz and is spectrally reversed. The “Digital IF” (DIF) FPGA module downconverts this to 0 Hz (so now the samples are complex-valued), filters to 50 MHz bandwidth, decimates by 2, and then upconverts to a center frequency of +25 MHz (still complex). The data emerges from the DIF module in 16-bit “I” + 16-bit “Q” format at 100 MSPS. The same process is applied to a separate, independently-tunable 50-MHz swath at L-Band, with the difference that the digital output is centered at -25 MHz. The two 50 MHz bands are simply added together to form a single 100 MHz bandwidth signal.

Following the DIF output is a cascade of FPGA modules which can be programmed to perform a variety of functions. Our favored strategy currently is as shown in Figure 1: mitigation of radar pulses using asynchronous pulse blanking (APB, described below), channelization into 100-kHz bins using a 1K FFT, frequency domain blanking, and integration to generate power spectra.

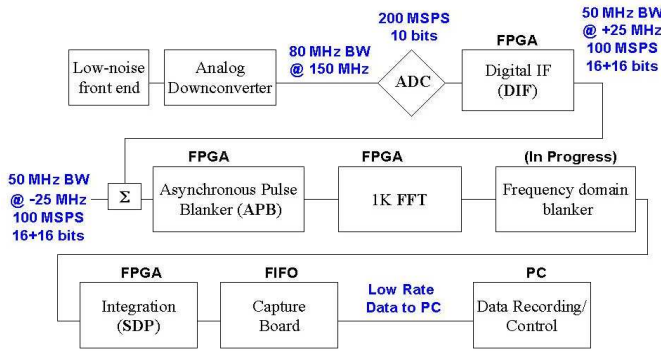


Figure 1. Block diagram of radiometer.

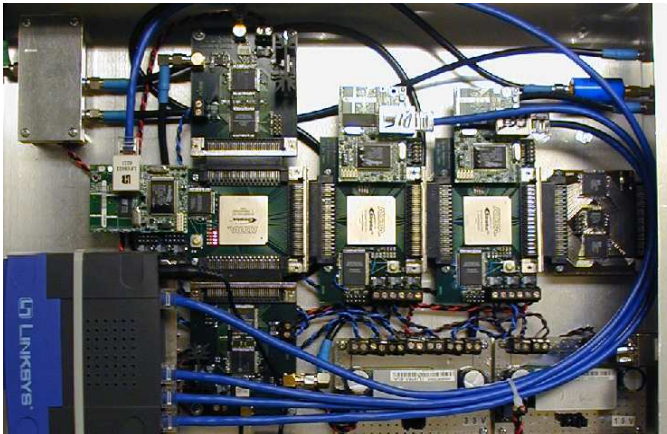


Figure 2. Digital backend; the vertical cascade of three circuit boards near the left hand side contains the dual ADC sections (upper and lower boards) and the digital channel combination and filtering section (center board). The APB section for removing temporal pulses is also implemented on the center board. Following the vertical cascade to the right is the FFT processor, then the SDP section for power computation and integration operations. Finally a “capture card” provides the interface to the PC. Microcontrollers are also included on each card (the smaller attached circuit boards with ethernet cables) to enable PC setting of internal FPGA parameters through an ethernet interface.

The APB is designed to detect and blank radar pulses, which typically are the dominant source of external L-Band RFI below 1400 MHz. Radar pulses range from 2–400 μs in length and occur 1–75 ms apart [2]. To detect these pulses, the APB maintains a running estimate of the mean and variance of the sample magnitudes. Whenever a sample magnitude greater than a threshold number of standard deviations from the mean is detected, the APB blanks (sets to zero) a block of samples beginning from a predetermined period before the triggering sample, through and hopefully including any multipath components associated with the detected pulse. (A future version of this algorithm will probably implement some form of matched filtering to improve detection performance.) APB operating parameters are adjustable and can be set by the user; see Section 3 for an example.

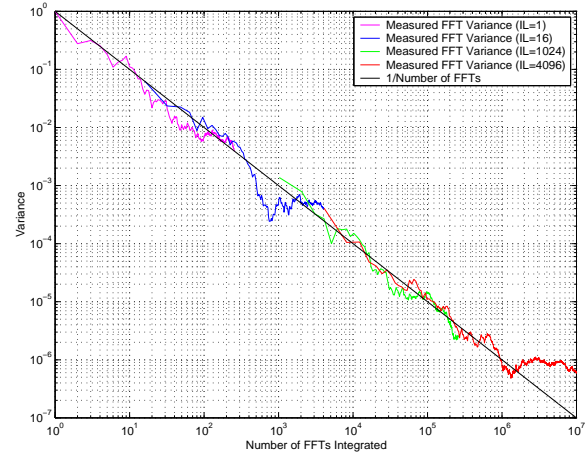


Figure 3. Noise variance vs. time for the radiometer when terminated by a matched load at the input. This observation represents 100 s of integration over 14 min elapsed time. No calibration, temperature control, or Dicke switching of any kind was employed.

Following the APB is a length-1K complex FFT, which achieves approximately 98% duty cycle in performing the FFT computations. A triangular window is applied before the FFT. Planned but not yet implemented is a frequency-domain blanking module, which is similar in concept to the APB, except applied independently to each frequency bin. The purpose of this module will be to exploit the processing gain achieved through channelization to detect and excise weak, relatively narrowband RFI. The FFT output is processed through a “spectral domain processor” (SDP) module which computes magnitude-squared for each frequency bin and computes a linear power average over many FFT outputs. These results are passed at a relatively low rate to a PC via a capture board. Total power can be computed by summation of frequency bins within the digital hardware, or the same process can be implemented within the PC for increased flexibility in monitoring RFI, selecting subbands, and so on.

Beyond considerations of RFI mitigation, this architecture has additional advantages over traditional radiometers. Because the noise level is positioned in the low-order bits of the A/D (primarily to allow headroom for strong RFI), only about 50–60 dB gain is required from the front end. Relative to radiometers requiring 100 dB or more of front end gain, this dramatically improves stability in the presence of temperature variations. Also, the final 50-MHz-wide IF filter is digital, and significantly narrower than the final analog filter, which is 80 MHz wide. Figure 3 demonstrates results from an initial stability test of this design through observation of an ambient temperature load (not thermally stabilized.) Near ideal performance of the system is observed as the integration period is increased from approximately 10 μsec up to approximately 10 sec. The real time elapsed during this measurement was approximately 14 minutes.

3. ON-THE-AIR TESTING AT ARECIBO

In November 2002, we had an opportunity to test the RFI mitigation capabilities of the radiometer by “piggybacking” on a radio astronomical observation at the Arecibo (Puerto Rico) Observatory. L-band radio astronomy, like remote sensing, is plagued by RFI; in particular, interference from radars in the 1215–1400 MHz band. Our radiometer was connected to the telescope through a spare IF output at ~ 250 MHz, which we upconverted back to L-band for input into our system. At the time, we had only one of the two 50 MHz subbands constructed. The SDP was configured to compute linear power averages over 4096 length-1K FFT outputs, for an effective integration time of ~ 42 ms. After 254 of these spectra were collected in a FIFO, the data were transferred to the PC and the experiment terminated.

The APB was configured as follows:

- Trigger on sample magnitudes greater than $\sim 10\sigma$ above the mean.
- Start blanking 100 samples ($1 \mu\text{s}$) in advance of the triggering sample.
- Blanking period is $100 \mu\text{s}$ long.
- Wait at least $44 \mu\text{s}$ between triggers (attempting to prevent multiple triggers on the same pulse).

These parameters were selected based on some known properties of a strong radar visible at Arecibo [3], and no attempt was made to optimize these parameters based on the observed data.

Measurements were taken at three center frequencies: 1255 MHz, 1300 MHz, and 1350 MHz; in each case, we performed the measurement once with the APB disabled, and then again with the APB on. The 1350 MHz results are shown in Figure 4. These spectra represent ~ 10.7 s of integration in ~ 42 ms segments evenly distributed over ~ 56 s in real time. Also shown in Figure 4 is the “max hold” of the 42-ms spectra. The max hold spectra are computed by taking for each frequency bin the maximum value observed in that bin over the course of the experiment. Max hold spectra are useful for revealing bursty signals (especially radars) which tend to be suppressed in deep integrations due to their low duty cycle.

With the APB off, we observe strong RFI at 1330 and 1350 MHz (these are in fact transmitted from the same radar), plus a few other frequencies. The front end of the telescope’s receiver is driven into compression when the 1330/1350 MHz radar is pointed near Arecibo, which occurs every ~ 11 s and accounts for the ragged max hold spectrum. When the APB is turned on, we see a dramatic improvement in the sense that large portions of the spectrum are salvaged. In this case, we found that $\sim 5\%$ of the data was blanked by the APB.

Note that 1330/1350 MHz radar is not completely suppressed by the APB. The reason for this is that the version of the APB algorithm used here assumes that only one radar is present at

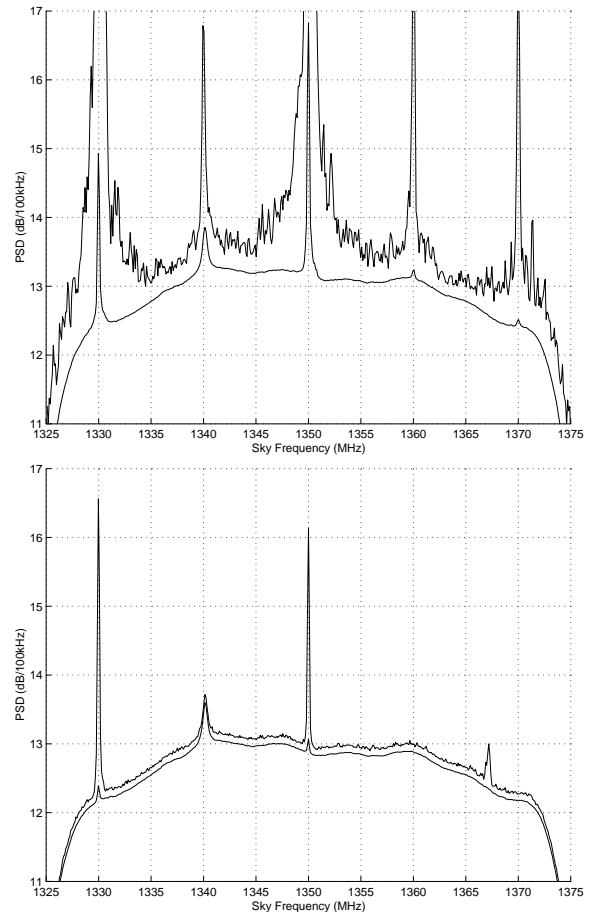


Figure 4. Mean and max-hold spectra. *Top Panel:* APB off; *Bottom panel:* APB on.

a time. As a result, a relatively weak radar pulse can distract the APB from a stronger radar pulse occurring later within the specified blanking period. This shortcoming is currently being corrected.

Figure 5 shows total power in 50 MHz bandwidth as a function of time. The ~ 11 s rotation period of the 1330/1350 MHz radar is clearly evident in the APB-off data. When the APB is turned on, the radar appears to be completely removed. The performance appears to be better in this case because the residual shown in the lower panel of Figure 4 is limited to a very small fraction of the processed time-frequency space, and thus becomes insignificant compared to the total noise power available in the band. We conclude that even simple blanking schemes as used here show great promise for use in total-power radiometry. Further results from these experiments are available in [4].

4. REMOTE SENSING EXPERIMENTS

To demonstrate performance of the system for Earth remote sensing, a series of ground-based experiments are currently in progress. These experiments involve observation of a water pool from the roof of the ElectroScience Laboratory at Ohio State University. Figure 6 illustrates the experiment config-

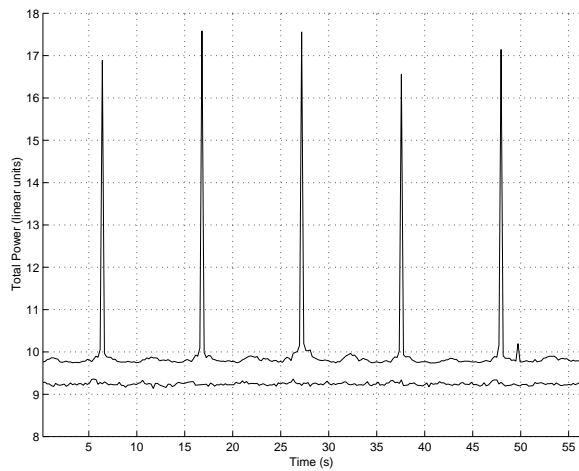


Figure 5. Time domain total power. *Top:* APB off; *Bottom:* APB on.

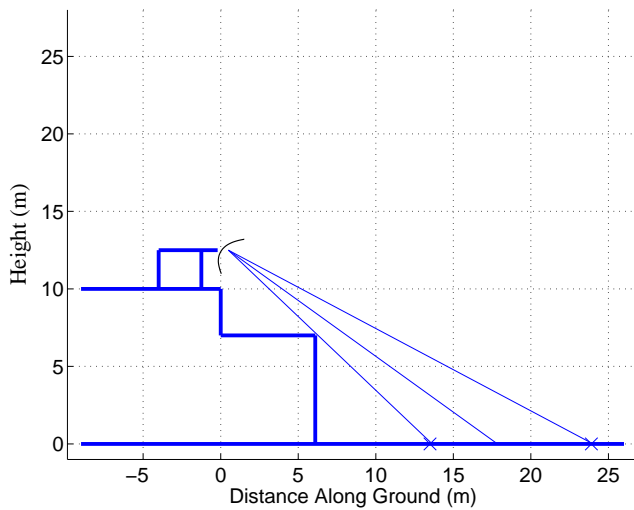


Figure 6. Geometry of ground-based remote sensing experiments.

uration; a 1.2 m reflector antenna is operated from approximately an 11.5 m height above the ground. This geometry results in far-field observations of the water pool when observed at approximately 53 degrees incidence. After pattern tests were performed to locate the antenna spot center on the ground, a water pool of dimensions 4.87 m by 9.75 m by 0.23 m depth was constructed. This area approximately covers the 3-dB spot of the antenna, and the depth is sufficient so that no significant contributions from below the pool are observed with water of 10 psu salinity or greater. Figure 7 is a photograph of the antenna as deployed.

External calibration of these measurements is performed by covering the entire pool area with microwave absorbing and reflecting materials successively. Figure 8 illustrates the pool when covered with absorbers or reflectors, and when uncovered. Under the assumption that the absorber presents a brightness equal to that of its physical temperature, and that



Figure 7. Photograph of antenna deployed on Electro-Science Laboratory roof

the sky brightness is known, these two targets can serve as an external calibration so that the water surface brightness can be determined. By using calibration targets exactly the same size as the water pool, contributions from antenna sidelobes surrounding the pool remain constant in the three measurements, so that a reasonable calibration should be possible. Because the L-band brightness temperature of a flat water surface can be accurately predicted from knowledge of its physical temperature and salinity [5], comparison of the measurement results with the predicted values will allow tests of the radiometric performance achieved by the system in the presence of RFI.

Note in Figure 7 that the L-band front-end is attached to the circular waveguide feed used to excite the reflector antenna. This front-end is temperature controlled to within 0.1 C, and contains both a noise generator and temperature controlled terminator as internal calibration standards. The front-end also contains a 1250-1500 MHz filter coupled through an isolator to the system LNA. The front-end is connected to the remaining analog-downconverter components inside the laboratory by approximately 20 m of coaxial cable (loss approximately 7 dB). While temperature control of the front-end is critical to maintain the accuracy of the internal calibration standards, no temperature control is implemented in the system beyond the front-end. Detailed tests of the resulting system stability are currently in progress; initial results indicate that the gain remains sufficiently stable for remote sensing purposes over at least a period of one hour without repeated external calibration.

Although the RFI environment in a ground-based experiment is generally expected to be less challenging than that in an aircraft- or space-based experiment (due to the more rapid increase in loss versus distance for ground-based links), the environment of these experiments remains difficult. The pri-

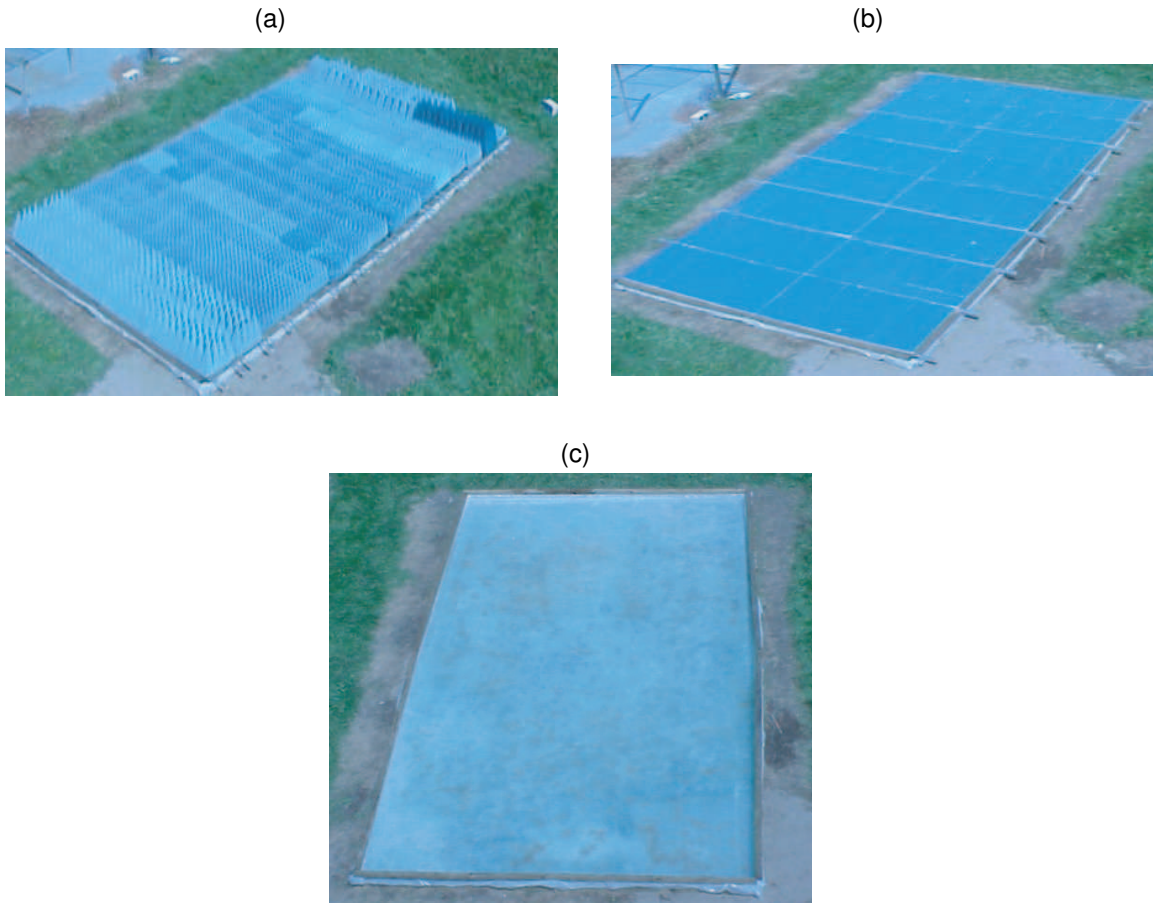


Figure 8. Water pool (a) covered with absorber (b) covered with reflecting material, and (c) uncovered

major interference source is an air-traffic control radar located approximately 40 km away in London, OH. Observations show a center frequency of 1331 MHz, with pulse lengths of approximately $2 \mu\text{sec}$ repeated every 2.85 msec. Experiments are being performed in the band 1325-1425 MHz in order to capture both this interferer and portions of the protected L-band spectrum. Other interferers, of both pulsed and continuous wave types, have also been observed, although on a more inconsistent basis.

Although data from these experiments are currently being analyzed, preliminary results again show the ability of the APB processor in reducing pulsed interference. Figure 9 illustrates 21 msec integrated FFT power outputs from 1325-1425 MHz as a function of observation time for the absorber target in horizontal polarization. Results in plot (a) were obtained with the APB section off, while plot (b) results had the APB section on, using parameters similar to those in the Arecibo measurement. The local air-traffic control radar at 1331 MHz is clearly visible with the blanker off, along with the occasional corruption of the entire spectrum caused by this radar. Other sporadic interference within the protected band is also observed with the APB off. Both these effects are greatly reduced with the APB section on, so that radiometry becomes more feasible in this portion of the spectrum. Of course, some interference remains, so that further processing of the results

is required to continue to improve system performance. The smaller variations observed across frequency represent the system gain response, and will be corrected through the external calibration procedure. The darker region in particular near 1375 MHz is located in the cross-over region of the two 50 MHz channels.

5. RFI SURVEYS

While initial results from the Arecibo and ground-based measurements are promising, further improvements should be possible through appropriate choices of the parameters of the RFI mitigation algorithms. Choosing these parameters as well as designing new mitigation strategies requires detailed information on properties of the RFI environment. Information on the RFI environment over a range of geographical locations is also of interest for developing and testing mitigation strategies for a future satellite borne sensor.

To address this issue, surveys of RFI in the frequency range 1200-1800 MHz have been performed from an airborne platform. The data were collected using a portable instrument known as the L-Band Interference Surveyor/Analyzer (LISA), which was developed at the Ohio State University ElectroScience Laboratory in 2002 [6]. LISA can include up to two complementary subsystems: an off-the-shelf

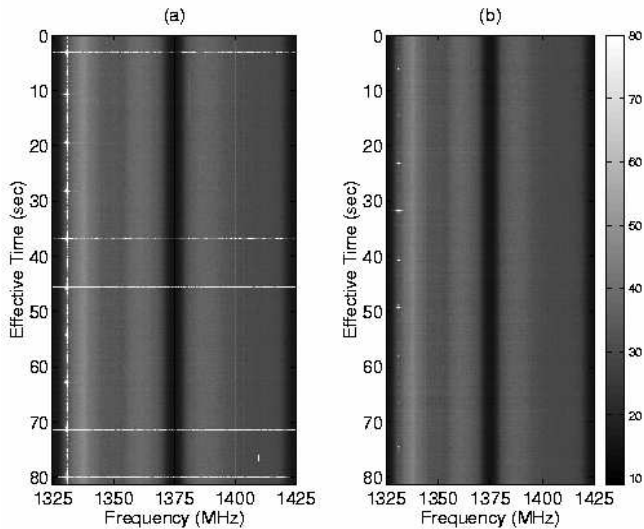


Figure 9. Integrated FFT power outputs from observation of absorber target in horizontal polarizations. APB off in plot (a), on in plot (b)

computer-controlled spectrum analyzer and a custom wide-band high-dynamic-range coherent-sampling receiver. The former is useful for understanding the distribution of RFI over large frequency spans and long time periods, whereas the latter provides waveform capture capability with high temporal resolution. To date the LISA instrument has acquired data in 14 flights, including an initial test flight above the mid-Atlantic coast [7], a flight from the Wallops Flight Facility in Virginia to Monterey, California, flights over the Pacific ocean from Monterey to Kona, Hawaii, and from Wake Island to Yokota Japan, and 10 flights over regions in the vicinity of Japan [8]. The latter flights occurred as part of the “Wakasa Bay” campaign in Japan to serve as a validation of AMSR-E meteorological measurements. Although the digital receiver backend of the radiometer discussed in Section 2 can also provide waveform capture capability, the LISA wideband receiver was based on an earlier radio-astronomy system due to time and scheduling issues.

Analysis of the data from these measurements shows that several interference types were observed, including numerous air-traffic control radars similar to those previously discussed, other radars, and communication systems. Results also suggest that a simple $1/R^2$ propagation law is typically reasonable for predicting expected RFI levels to be observed from air- or space- platforms. Technical reports [7]-[8] including further details about LISA and the resulting data are available from the authors.

Developing interference mitigation methods for C-band radiometers will also require an improved knowledge of the C-band RFI environment. Although some information is available from aircraft- [9] and space-based [1] radiometers, the temporal and spectral resolution of this data is insufficient

to provide detailed signal properties. To address this issue, a project has been initiated to operate the digital receiver described in Section 2 at C-band in aircraft measurements. These measurements will be performed in collaboration with the Environmental Technology Laboratory of NOAA, by use of the Polar Scanning Radiometer (PSR) system [9] as the “front-end” in these experiments. Results from these measurements will indicate the degree to which the APB section is successful at C-band, as well as provide new information on the C-band RFI environment.

6. IMPLICATIONS

Current results of the project suggest that simple time- and/or frequency blanking strategies can allow radiometric measurements in many portions of the spectrum. For L-band in particular, the predominance of air-traffic control radars makes time-blanking an effective strategy. The measurements currently in progress should provide an indication as to the degree to which radiometric accuracy is impacted by active RFI suppression. Updated results from these experiments will be presented at the conference. Finally, continued surveys of the RFI environment remain important, so that mitigation algorithms can be continually refined and updated as new source information is obtained.

ACKNOWLEDGMENTS

The authors are grateful for the assistance of E. Kim of NASA/GSFC and D. Easmunt of Dyncorp (at NASA/WFF) for their assistance in the logistics and conduct of these measurements. This work was supported in part by NASA “Instrument Incubator Program” project NAS5-02001 and in part by the National Science Foundation (NSF) under Award No. AST-0138263. Thanks to J. Cordes, R. Bhat, P. Perillat, and L. Wray for advice and technical support at Arecibo. The Arecibo Observatory is operated by Cornell University under a Cooperative Agreement with the NSF.

REFERENCES

- [1] Li, L., E. Njoku, E. Im, P. Chang, and K. St.Germain, "A preliminary survey of radio-frequency interference over the US in Aqua AMSR-E data," accepted by *IEEE Trans. Geosc. Rem. Sens.*, 2003.
- [2] S.W. Ellingson, *Characterization of Some L-Band Signals Visible at Arecibo*, Technical Report 743467-2, The Ohio State University ElectroScience Laboratory, February 2003.
- [3] S.W. Ellingson and G.A. Hampson, "Mitigation of Radar Interference in L-Band Radio Astronomy," *Astrophysical J. Supp.*, vol. 147 (1), pp. 167–176, 2003.
- [4] S.W. Ellingson and G.A. Hampson, *RFI and Asynchronous Pulse Blanking in the 1230-1375 MHz Band at Arecibo*, The Ohio State University ElectroScience Laboratory Technical Report 743467-3, Feb 2003.
- [5] W. J. Wilson, S. H. Yueh, S. Dinardo, and F. Li, "L/S-band radiometer measurements of a saltwater pond," *Proc. 2002 IGARSS*, vol. 2, pp. 1120-1122, Toronto.
- [6] S. W. Ellingson, G. A. Hampson, and J. T. Johnson, "Characterization of L-band RFI and Implications for Mitigation Techniques," *Proc. 2003 IGARSS*, Toulouse.
- [7] S. W. Ellingson and J. T. Johnson, *Airborne RFI Measurements over the Mid-Atlantic Coast using LISA*, Technical Report, The Ohio State University ElectroScience Laboratory, January 2003.
- [8] J. T. Johnson and S. W. Ellingson, *Airborne RFI Measurements Using LISA During Transit to and in the Wakasa Bay Campaign*, Technical Report, The Ohio State University ElectroScience Laboratory, July 2003.
- [9] Gasiewski, A. J., M. Klein, A. Yevgrafov, and V. Leuski, "Interference mitigation in passive microwave radiometry," *Proc. 2002 IGARSS*, Toronto.

Grant A. Hampson is a Research Scientist in the Department of Electrical Engineering and ElectroScience Laboratory of The Ohio State University, Columbus, OH. His research interests include digital systems design and efficient beamforming architectures. He received the B. Sc. and Ph.D. degrees in computing from Monash University, Melbourne, Australia, in 1993 and 1997, respectively.

Steven W. Ellingson is an Assistant Professor in the Bradley Department of Electrical and Computer Engineering, Virginia Polytechnic Institute and State University, Blacksburg, VA. His research interests include antennas and propagation, applied signal processing, and RF system design. Dr. Ellingson received the B.S. degree in Electrical and Computer Engineering from Clarkson University, Potsdam, NY, in 1987, and

the M.S. and Ph.D. degrees in Electrical Engineering from the Ohio State University, Columbus, OH, in 1989 and 2000, respectively.

Joel T. Johnson is an Associate Professor in the Department of Electrical Engineering and ElectroScience Laboratory of The Ohio State University, Columbus, OH. His research interests include microwave remote sensing, applied electromagnetics, and rough surface scattering. He is the author of 50 articles in the areas indicated above. Dr. Johnson obtained the M.S. and Ph.D. degrees in electrical engineering from the Massachusetts Institute of Technology in 1993 and 1996, respectively. He is a member of IEEE and URSI commissions B and F.